

Superdiffusive transport in quasi-particle dephasing models

Yu-Peng Wang^{1,2}, Chen Fang^{1,3,4} and Jie Ren^{1,2*}

1 Beijing National Laboratory for Condensed Matter Physics and Institute of Physics, Chinese Academy of Sciences, Beijing 100190, China

2 University of Chinese Academy of Sciences, Beijing 100049, China

3 Songshan Lake Materials Laboratory, Dongguan, Guangdong 523808, China

4 Kavli Institute for Theoretical Sciences, Chinese Academy of Sciences, Beijing 100190, China

* jiere@iphy.ac.cn

Abstract

Investigating the behavior of noninteracting fermions subjected to local dephasing, we reveal that quasi-particle dephasing can induce superdiffusive transport. This superdiffusion arises from nodal points within the momentum distribution of local dephasing quasi-particles, leading to asymptotic long-lived modes. By studying the dynamics of the Wigner function, we rigorously elucidate how the dynamics of these enduring modes give rise to Lévy walk processes, a renowned mechanism underlying superdiffusion phenomena. Our research demonstrates the controllability of dynamical scaling exponents by selecting quasi-particles and extends its applicability to higher dimensions, underlining the pervasive nature of superdiffusion in dephasing models.

Copyright attribution to authors.

This work is a submission to SciPost Physics Core.

License information to appear upon publication.

Publication information to appear upon publication.

Received Date

Accepted Date

Published Date

1

2 Contents

3	1 Introduction	2
4	2 Quasi-Particle Dephasing Model	3
5	3 Theoretical Prediction of the Dynamical Exponent	5
6	3.1 Wigner dynamics	5
7	3.2 Lévy walk	6
8	4 Spectrum of Exact Dynamical Critical Exponents	8
9	4.1 Fine-tuning the dephasing quasi-particles	8
10	4.2 Higher Dimensional Cases	9
11	5 Conclusion	11
12	A Closed Hierarchy of the Correlation Function	12
13	B Effective Hydrodynamics	13

14	C Comparison between Exact Lindblad and Wigner Dynamics	17
15	References	17

16
17

18 1 Introduction

19 Transport properties of particles, energy, and information in nonequilibrium quantum many-
20 body systems have garnered significant attention [1–12]. The emergence of anomalous trans-
21 port, which deviates from the classical diffusion characterized by linear growth in mean square
22 displacement over time, challenges established principles in quantum many-body dynamics.
23 This anomaly includes superdiffusion [13] and subdiffusion [14], where particle spreading
24 occurs faster or slower than classical expectations.

25 Notably, the one-dimensional Heisenberg model has exhibited superdiffusion [15–22] with
26 a dynamical exponent of $z = 3/2$ and a scaling function within the Kardar-Parisi-Zhang (KPZ)
27 universality class [23–25]. This superdiffusive behavior extends to a broader class of integrable
28 models with non-Abelian symmetries [26–31], with transitions to diffusive behavior observed
29 when integrability or symmetry is perturbed [32–35]. Superdiffusion has also been identified
30 in systems with long-range interactions [36–41] and short-range interacting systems subject
31 to quasiperiodic potentials [42, 43], albeit with some controversies [44].

32 So far, the study of superdiffusion mainly focuses on closed systems since it is generally
33 believed that coupling a system to the environment results in bulk dissipation, leading to dif-
34 fusion. A well-studied example is the free fermion chain subject to local particle dephasing
35 [45–51]. In this context, dephasing introduces finite lifetimes to the original free modes,
36 resulting in a mean free path beyond which particle motion resembles a Gaussian random
37 walk.

38 In contrast, our study identifies a superdiffusive transport in noninteracting fermion sys-
39 tems by generalizing the onsite dephasing to “quasi-particle” dephasing. The “quasi-particles”
40 are defined as superpositions of fermions near position x :

$$\hat{d}_x = \sum_a d_a \hat{c}_{x+a}, \quad (1)$$

41 where the vector d_a is assumed to be local near the origin. The momentum distribution char-
42 acterizing these quasi-particles is

$$d_k \equiv \sum_a d_a e^{ika}. \quad (2)$$

43 Remarkably, our investigation unveils a direct link between the nodal structure of d_k and the
44 occurrence of superdiffusion:

- 45 1. When d_k possesses a nodal point at generic momentum k_o (with nonzero velocity $v_{k_o} \neq 0$)
46 characterized by $|d_k| \sim (k - k_o)^n$, particle transport exhibits a ballistic front, and the
47 dynamical scaling exponent is given by $z_n = (2n + 1)/(2n)$;
- 48 2. In cases where d_k features a higher-order nodal point at zero-velocity point k_o , described
49 as $|d_k| \sim (k - k_o)^n$ where $n \geq 2$, the particle transport exhibit a superdiffusive front,
50 and the dynamical exponent is $z_n = (2n + 1)/(2n - 1)$.

51 We demonstrate the superdiffusion in dephasing models by analyzing the dynamics of the
52 Wigner function [50, 51]. This approach develops a hydrodynamics description effective in

53 capturing transport behavior across extended temporal and spatial scales. The hydrodynamics
 54 framework translates the many-body transport problem into a single-particle random walk
 55 process. In this context, the presence of nodal points signifies the existence of long-lived modes
 56 with diverging mean free paths. The probabilistic distribution characterizing these mean free
 57 paths exhibits a heavy-tailed nature, a hallmark of the Lévy walk [52], a well-established model
 58 of superdiffusive processes.

59 Significantly, the dynamical exponent of the charge transport is intricately linked to the
 60 nodal structure of the dephasing quasi-particle. In instances where certain symmetries are
 61 present, the presence of nodal points becomes generic, leading to a robust manifestation of
 62 superdiffusion characterized by exact dynamical exponents. Besides, fine-tuning the nodal
 63 structure of quasi-particles enables the systematic generation of a spectrum of dynamical expo-
 64 nents. Our analytical approach extends naturally to higher-dimensional systems, underscoring
 65 the universality of our findings in the context of dephasing models.

66 2 Quasi-Particle Dephasing Model

67 Consider the dynamics of a dephasing model governed by the Lindbladian:

$$\partial_t \hat{\rho} = -i[\hat{H}, \hat{\rho}] - \frac{\gamma}{2} \sum_x [\hat{L}_x, [\hat{L}_x, \hat{\rho}]], \quad (3)$$

68 where the Hamiltonian \hat{H} represents a basic noninteracting fermion chain, given by

$$\hat{H} = \sum_i (\hat{c}_i^\dagger \hat{c}_{i+1} + \hat{c}_{i+1}^\dagger \hat{c}_i), \quad (4)$$

69 characterized by a group velocity $v_k = 2 \sin k$. The jump operator $\hat{L}_x = \hat{d}_x^\dagger \hat{d}_x$ captures the
 70 dephasing process affecting the quasi-particles \hat{d}_x . In the previous studies, particularly in the
 71 context of both monitored [50] and open systems [46], the case where $\hat{d}_x = \hat{c}_x$ has been
 72 well-explored, resulting in a clear demonstration of diffusive particle transport.

73 We first focus on the scenario involving quasi-particles with time-reversal and spatial-
 74 reflection symmetry. Specifically, we examine a scenario involving a three-site quasi-particle
 75 configuration:

$$\hat{d}_x = \frac{1}{\sqrt{2+a^2}} (\hat{c}_{x-1} - a \hat{c}_x + \hat{c}_{x+1}), \quad (5)$$

76 where a is a real parameter. The corresponding momentum distribution is

$$d_k = \frac{2 \cos k - a}{\sqrt{2+a^2}}. \quad (6)$$

77 In the range $-2 < a < 2$, d_k exhibits two nodal points, $k_\pm = \pm \arccos(a/2)$, around which d_k
 78 is linearly dispersed. Upon reaching $a = \pm 2$, these two nodal points merge into a higher-order
 79 nodal point at $k = 0$ or $k = \pi$ with quadratic dispersion: $d_k \propto \sin^2(k/2)$. For values $|a| > 2$,
 80 d_k does not possess any nodal point.

81 Starting from a half-filling domain wall state

$$|\psi_o\rangle = |1 \dots 1 0 \dots 0\rangle, \quad (7)$$

82 we study the evolution of the particle density $\langle \hat{n}_i \rangle_t = \langle \hat{c}_i^\dagger \hat{c}_i \rangle_t$ as well as the transported charge
 83 $C(t) = \sum_{i \geq 1} \langle \hat{n}_i \rangle_t$ by computing the dynamics of the two-point correlation function $\langle \hat{c}_i^\dagger \hat{c}_j \rangle$
 84 under Eq. (3). The Lindbladian with quadratic Hermitian jump operator \hat{L} satisfies a closed

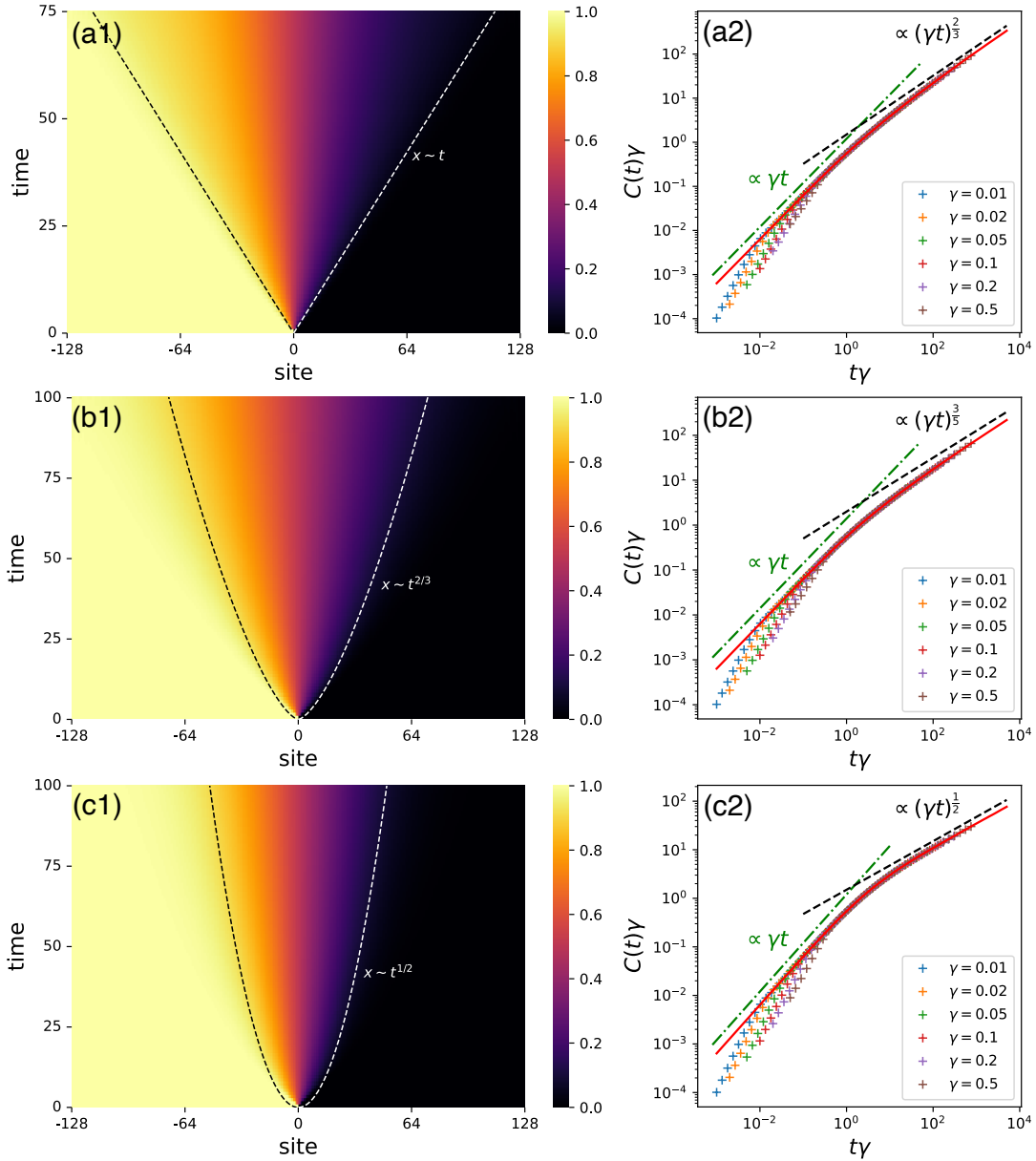


Figure 1: Numerical simulations of the particle transport of the dephasing Lindbladian Eq. (3), with \hat{d}_x defined according to Eq. (5). Subplots are presented for different parameters, namely (a1)(a2) for $a = \sqrt{2}$, (b1)(b2) for $a = 2$, and (c1)(c2) for $a = 3$. Subplots (a1)(b1)(c1) display the density evolution of systems with different dephasing quasi-particles. The system sizes are fixed to $L = 256$, and the dephasing strength is $\gamma = 0.5$. The dynamics are initiated from the domain-wall state $|\psi_o\rangle = |1 \dots 10 \dots 0\rangle$, and feature either (a1) a ballistic wavefront, (b1) a superdiffusive wavefront, or (c1) a diffusive wavefront. Subplots (a2)(b2)(c2) shows the charge transport $C(t)$ for different dephasing quasi-particles. The system size for this simulation is fixed to $L = 3000$. For exact Lindbladian simulation, in the short time regime ($t < 1$), the transport behaviors deviate from the hydrodynamics results, following a $C(t) \propto t^2$ scaling. After $t > 1$, the Lindbladian result approaches the hydrodynamics, which exhibits a crossover from ballistic ($z = 1$) to (a2) superdiffusive with dynamical exponent $z = 3/2$, (b2) superdiffusive with dynamical exponent $z = 5/3$, and (c2) diffusive with dynamical exponent $z = 2$.

85 hierarchy [53–55]. In this case, the evolution equation of $\langle \hat{c}_i^\dagger \hat{c}_j \rangle$ is closed (see Appendix A
 86 for deriving the correlation function dynamics). Therefore, we can numerically simulate the
 87 charge transport for system size up to $L = 3000$. For different choices of \mathbf{a} , there are three
 88 distinct transport behaviors.

89 **$\mathbf{a} = \sqrt{2}$ case** From Fig. 1(a1), we see the density evolution features a ballistic front. The
 90 charge transport shows a scaling behavior (after $t > 1$):

$$\gamma C(t) \sim f(\gamma t), \quad (8)$$

91 wherein the scaling function exhibits asymptotic behavior:

$$f(x) \sim x^{2/3} \quad \text{as } x \rightarrow \infty.$$

92 This behavior indicates a dynamical exponent converging to

$$z = \frac{3}{2} \quad (9)$$

93 in the long-time regime. Note that the scaling function does not conform to the KPZ univer-
 94 sality class due to a ballistic wavefront.

95 **$\mathbf{a} = 2$ case** As shown in Fig. 1(b1), the density evolution exhibits a superdiffusive front
 96 instead. After $t > 1$, the transport converges to the form [displayed in Fig. 1(b2)]

$$\gamma C(t) \sim g(\gamma t), \quad (10)$$

97 with a different scaling function

$$g(x) \sim x^{3/5}$$

98 in the large x limit, indicating a dynamical exponent of

$$z = \frac{5}{3}. \quad (11)$$

99 **$\mathbf{a} = 3$ case** As demonstrated in Fig. 1(c1) [and in Fig. 1(c2) regarding the dynamical expo-
 100 nent], the transport displays apparent diffusive scaling in the long-time regime.

101 This observation underscores the close relationship between the nodal structure of the
 102 dephasing quasi-particle and the dynamical scaling of the transport.

103 3 Theoretical Prediction of the Dynamical Exponent

104 3.1 Wigner dynamics

105 In Refs. [50, 51], the authors introduced a hydrodynamics framework tailored for free fermion
 106 systems characterized by quadratic jump operators. The hydrodynamics of the free fermion
 107 system is captured by the Wigner distribution [56]:

$$n(x, k, t) \equiv \sum_s e^{iks} \left\langle \hat{c}_{x+s/2}^\dagger \hat{c}_{x-s/2} \right\rangle_t. \quad (12)$$

108 This quantity essentially represents the particle density at position \mathbf{x} with momentum \mathbf{k} and
 109 offers a semiclassical perspective that accurately captures the system's dynamics in a coarse-
 110 grained sense. In Appendix B, we formally prove the exact Lindblad equation (3) leads to the
 111 following Wigner dynamics:

$$\frac{\partial n}{\partial t}(\mathbf{x}, \mathbf{k}, t) = -2 \sin k \frac{\partial n}{\partial x}(\mathbf{x}, \mathbf{k}, t) - \gamma |\mathbf{d}_k|^2 n(\mathbf{x}, \mathbf{k}, t) + \gamma |\mathbf{d}_k|^2 \int \frac{d\mathbf{q}}{2\pi} |\mathbf{d}_q|^2 n(\mathbf{x}, \mathbf{q}, t). \quad (13)$$

112 This equation describes a statistical process wherein a wave packet with momentum \mathbf{k} has a
 113 probability proportional to $|\mathbf{d}_k|^2$ to shift to a different momentum. The probability distribution
 114 of the new momentum \mathbf{q} follows the distribution $|\mathbf{d}_q|^2$. We proceed to solve this linear equation
 115 employing the Green's function method:

$$n(\mathbf{x}, \mathbf{k}, t) = (G * n_o)(\mathbf{x}, \mathbf{k}, t) = \int G(\mathbf{y}, \mathbf{k}, t) n_o(\mathbf{x} - \mathbf{y}, \mathbf{k}) d\mathbf{y}. \quad (14)$$

116 Taking the initial state as a domain wall configuration, i.e., $n_o(\mathbf{x}, \mathbf{k}) = \theta(-\mathbf{x})$, this expression
 117 simplifies to

$$n(\mathbf{x}, \mathbf{k}, t) = \int_x^\infty G(\mathbf{y}, \mathbf{k}, t) d\mathbf{y}, \quad (15)$$

118 with the initial condition $G(\mathbf{x}, \mathbf{k}, 0) = \delta(\mathbf{x})$. The Green's function $G(\mathbf{x}, \mathbf{k}, t)$ can be efficiently
 119 simulated via a random walk approach [50] involving the following steps:

- 120 1. The velocity is determined by momentum: $\mathbf{x}'(t) = \mathbf{v}[K(t)] = 2 \sin K(t)$.
- 121 2. The quantity $K(t)$ remains constant within each interval $[t_0, t_1), [t_1, t_2), \dots$, with each
 122 interval being independent and following an exponential distribution with an average
 123 value of $\overline{t_{i+1} - t_i} = \gamma^{-1} |\mathbf{d}_k|^{-2}$.
- 124 3. The momenta K_{i+1} are randomly distributed with a probability $p(\mathbf{k})$ proportional to
 125 $|\mathbf{d}_k|^2$.
- 126 4. The probability density $p(\mathbf{x}, \mathbf{k}, t)$ corresponds to the Green's function $G(\mathbf{x}, \mathbf{k}, t)$, which
 127 can be determined numerically by sampling various random trajectories.

128 By employing this method and sampling multiple random trajectories, we obtain access to the
 129 scaling exponent in the long-time regime with high accuracy.

130 For the specific dephasing model involving quasi-particles in Eq. (5), Fig. 1(a2)(b2)(c2)
 131 showcase comparisons of charge transport between the exact Lindbladian dynamics on a 1D
 132 lattice and the Wigner dynamics. Initially distinct, the Lindblad dynamics gradually converges
 133 to the Wigner dynamics beyond $t > 1$. In Appendix C, we demonstrate an agreement in the dy-
 134 namics of density profiles obtained through both methods, particularly evident in the long-time
 135 regime. This agreement supports the accuracy of the hydrodynamics description. Leveraging
 136 this validation, we extend our numerical simulation using Wigner dynamics, pushing the sim-
 137 ulation time to $t > 10^7$. As shown in Fig. 2, this extension enables a precise showcase of the
 138 convergence of the dynamical scaling $\alpha(t)$ towards $2/3$ and $3/5$.

139 3.2 Lévy walk

140 In the random walk picture, we show that the nodal point in the momentum distribution leads
 141 to the phenomenon of Lévy walk [52]. In stark contrast to the Gaussian characteristics defining
 142 Brownian motion and standard diffusion, a Lévy walk constitutes a stochastic process dictated

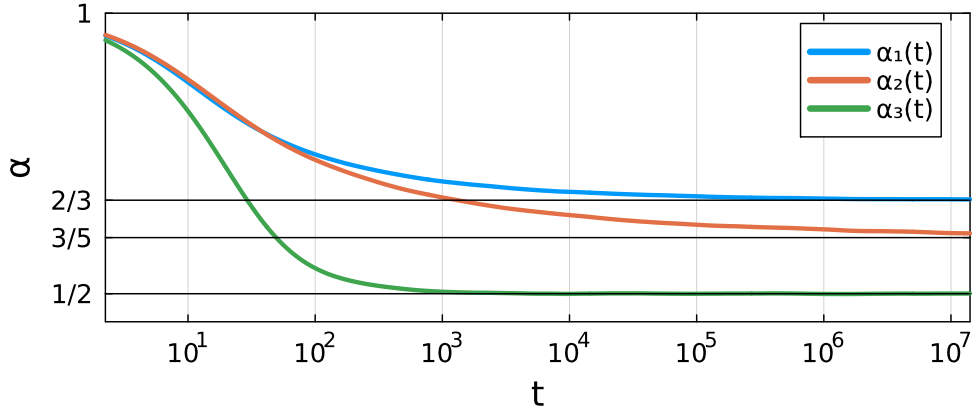


Figure 2: The dynamical exponent $\alpha(t) = d \log C(t) / d \log(t)$ of the charge transport for Wigner dynamics (13) with $\gamma = 0.1$. These results are obtained from the random walk simulations with 5×10^6 samples. The exponents $\alpha_1(t)$, $\alpha_2(t)$, and $\alpha_3(t)$ correspond to the cases $a = \sqrt{2}$, $a = 2$, and $a = 3$ respectively.

143 by a heavy-tailed probability distribution $p(l)$ governing step length l of each transition. In
 144 the $l \rightarrow \infty$ limit, this distribution conforms to a power-law behavior:

$$p(l) \sim l^{-1-z}, \quad (16)$$

145 where $1 < z < 2$ is the Lévy exponent. When each step takes equal time, the cumulative
 146 displacement conforms to an asymptotic behavior:

$$X(t) = \left| \sum_i l_i \right| \sim t^z. \quad (17)$$

147 Hence, the dynamical exponent governing the system's behavior aligns with the Lévy exponent,
 148 confirming that a Lévy walk implies superdiffusion.

149 In systems where time-reversal and reflection symmetries are preserved, we define an in-
 150 dicator as

$$\nu = d_0 d_\pi, \quad (18)$$

151 which indicates a nontrivial condition when $\nu \leq 0$. For quasi-particles in Eq. (5), this corre-
 152 sponds to the range $-2 \leq a \leq 2$. A nontrivial $\nu < 0$ implies the existence of a nodal point at
 153 $\mathbf{k}_o \in (0, \pi)$. We refer to this nodal point as a "generic nodal point." By introducing $\mathbf{q} = |\mathbf{k} - \mathbf{k}_o|$,
 154 in the vicinity of $\mathbf{q} \approx 0$, the mean free path exhibits the asymptotic behavior:

$$l_k \sim \tau_k \sim |d_k|^{-2} \sim q^{-2}. \quad (19)$$

155 As \mathbf{q} approaches zero, the mean free path diverges. A change of variable ($q \rightarrow l$) in the
 156 probabilistic distribution results in:

$$1 = \int p(q) dq \sim \int q^2 dq \sim \int l^{-1} d(l^{-1/2}) \sim \int l^{-5/2} dl,$$

157 leading to a free path distribution $p(l) \sim l^{-5/2}$. Since the average time step is constant:

$$\overline{t_{n+1} - t_n} = \int_k p(k) \tau_k = \frac{1}{\gamma},$$

158 this random walk behavior aligns with a Lévy walk, characterized by an exponent of $z = 3/2$,
 159 consistent with our numerical simulations in Fig. 1(a2).

160 When $\nu = 0$, \mathbf{d}_k possesses a nodal point at one of the high symmetry points, \mathbf{k}_o , with a
 161 vanishing velocity

$$v_k \sim |k - k_o| = q.$$

162 The symmetry condition requires the dispersion of \mathbf{d}_k to be at least quadratic: $\mathbf{d}_k \sim q^2$. As a
 163 result, the mean free path scales as

$$l_k \sim v_k \tau_k \sim q^{-3}.$$

164 Then a change of variable ($q \rightarrow l$) leads to

$$1 = \int p(q) dq \sim \int q^4 dq \sim \int l^{-4/3} d(l^{-1/3}) \sim \int l^{-8/3} dl,$$

165 which yields $p(l) \sim l^{-8/3}$. The dynamical scaling exponent becomes $z = 5/3$, in accordance
 166 to Fig. 1(b2).

167 In cases where $\nu > 0$, there is typically no nodal point in \mathbf{d}_k , resulting in a bounded mean
 168 free time: $\tau_k \leq \tau_{\max}$, and subsequently, a finite mean free path $l \leq l_{\max}$, resulting in ordinary
 169 diffusive behavior with $z = 2$, as shown in Fig. 1(c2).

170 4 Spectrum of Exact Dynamical Critical Exponents

171 4.1 Fine-tuning the dephasing quasi-particles

172 Beyond the symmetric setting, we can also leverage specific fine-tuned dephasing quasi-particles
 173 to attain higher-order dispersion near the nodal points. This diversity in dispersion yields var-
 174 ious dynamical scaling behaviors.

175 Let us begin by considering a model with a single nodal point:

$$|d_k| \sim \sin^n [(k - k_o)/2].$$

176 This type of dispersion can be realized by selecting the following form for \hat{d}_x :

$$\hat{d}_x = \frac{1}{\sqrt{\mathcal{N}_n}} \sum_{a=0}^n e^{-iak_o} \hat{c}_{x+a}.$$

177 where \mathcal{N}_n is the normalization factor, with the explicit form

$$\mathcal{N}_n = \sum_{a=0}^n \binom{n}{a}^2 = \frac{4^n \Gamma(n + \frac{1}{2})}{\sqrt{\pi} \Gamma(n)}, \quad \Gamma(x) \text{ is the Gamma function.}$$

178 In this case, \hat{d}_x possesses a nodal point at \mathbf{k}_o , exhibiting n -th order dispersion. Following
 179 similar derivations, the mean free path for momentum- \mathbf{k} wave packet is given by $l_k \sim q^{2n}$,
 180 and the distribution takes the form:

$$p(l) \sim l^{-1} \frac{d}{dl} (l^{-1/2n}) = l^{-1-(2n+1)/2n}.$$

181 The dynamical scaling exponents that can be tuned in this scenario are given by

$$z_n = \frac{2n + 1}{2n}. \quad (20)$$

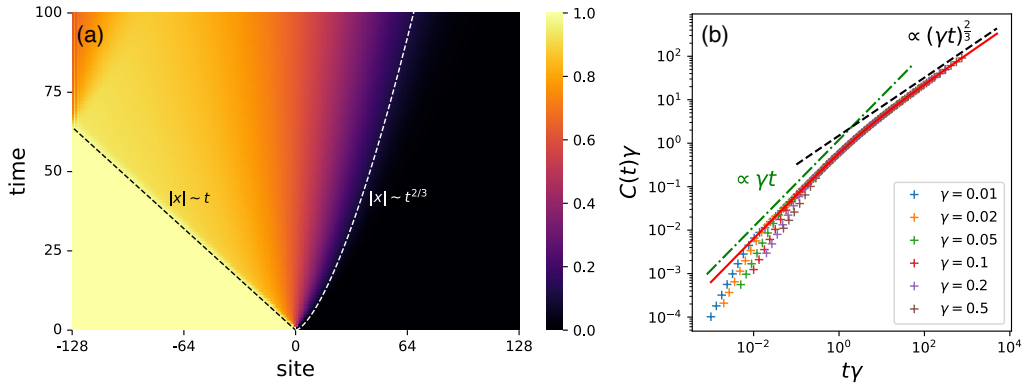


Figure 3: Numerical simulations of the (a) density evolution and the (b) particle transport of the quasi-particle dephasing system Eq. (3), with \hat{d}_x defined according to Eq. (21). (a) the density evolution features a ballistic wavefront for the left part and a superdiffusive front for the right part. Due to the difference in wavefront velocities, by $t = 100$, the left front has already reached the boundary, whereas the right front has not. (b) charge transport shows superdiffusive scaling with $z = 3/2$.

182 One simplest example is when $k_o = \pi/2$ and $n = 1$, in this case the dephasing quasiparticle
183 is

$$\hat{d}_x = \frac{1}{\sqrt{2}}(\hat{c}_x - i\hat{c}_{x+1}). \quad (21)$$

184 Note that since the dephasing quasi-particle has no reflection symmetry, the left and right
185 wavefronts are different, as displayed in Fig. 3(a). This behavior was previously observed in a
186 monitored free fermion system [57], which shows a special skin effect in the steady state when
187 adding certain feedback operations. The charge transport for this system shows superdiffusion
188 with $z = 3/2$.

189 On the other hand, if we set $k_o = 0$ (or equivalently $k_o = \pi$), the velocity $v_k \sim k$, resulting
190 in

$$l_k \sim v_k \tau_k \sim k^{-(2n-1)}.$$

191 Consequently, the probability distribution becomes:

$$p(l) \sim l^{-1-(2n+1)/(2n-1)},$$

192 which leads to the dynamical scaling exponent

$$z_n = \frac{2n+1}{2n-1}. \quad (22)$$

193 Note that the derivation is valid only for $n \geq 2$. In the $n = 1$ case, there would be usual
194 diffusive transport.

195 4.2 Higher Dimensional Cases

196 The analysis extends to higher dimensions, where nodal structures can also be nodal lines and
197 surfaces. To begin, the Wigner dynamics Eq. (13) naturally generalize to D -dimensions with
198 slight modifications:

$$\frac{\partial n}{\partial t}(\vec{x}, \vec{k}, t) = -2 \sum_{i=1}^D \sin(k_i) \frac{\partial n}{\partial x_i}(\vec{x}, \vec{k}, t) - \gamma |d_{\vec{k}}|^2 \left[n(\vec{x}, \vec{k}, t) - \int \frac{d^D q}{(2\pi)^D} |d_{\vec{q}}|^2 n(\vec{x}, \vec{q}, t) \right]. \quad (23)$$

199 We refer to Appendix B for the proof. For simplicity, we assume the systems to be square/cubic
200 lattices with nearest-neighbor hopping Hamiltonians, with dispersion relation

$$v_{\vec{k}} = 2(\sin k_1 + \sin k_2) \quad \text{and} \quad v_{\vec{k}} = 2(\sin k_1 + \sin k_2 + \sin k_3)$$

201 respectively.

202 **2D systems** If the dephasing quasi-particle has the time-reversal and reflection symmetry,
203 $d_{\vec{k}}$ is a real function on the Brillouin zone. We can then similarly define three independent
204 indicators:

$$v_1 = d_{(0,0)}d_{(\pi,0)}, \quad v_2 = d_{(0,0)}d_{(0,\pi)}, \quad \text{and} \quad v_3 = d_{(0,0)}d_{(\pi,\pi)}.$$

205 A negative value for these indicators indicates a nodal line $\vec{k}_o(\theta)$ in the Brillouin zone parametrized
206 by $\theta \in [0, 1)$. In proximity to this nodal line, we expect consistent behavior with $b_{\vec{k}} \sim k_{\perp}^n$,
207 where k_{\perp} represents the local variable orthogonal to the \vec{k}_o curve. The asymptotic probabilistic
208 distribution $p(k_{\perp})$ can be approximated by integrating out k_{\parallel} :

$$1 = \int p(\vec{k}) dk_{\parallel} dk_{\perp} \sim \int k_{\perp}^{2n} dk_{\perp}.$$

209 That is, $p(k_{\perp}) \sim k_{\perp}^{2n}$. The mean free path is then $l \sim k_{\perp}^{-2n}$, indicating a 2D Lévy walk with a
210 dynamical scaling exponent given by

$$z_n = \frac{2n + 1}{2n}. \quad (24)$$

211 The nodal line intersects with a high-symmetry point if any indicator yields zero. The transport
212 properties remain unchanged as they are determined by the segment of the curve with nonzero
213 momentum.

214 When we relax the symmetry restriction on \hat{d}_x , $d_{\vec{k}}$ becomes a complex function on \mathbf{k} . Even
215 in this case, nodal lines can exist without fine-tuning. Consider the winding number

$$W[C] = \oint_C \frac{d_{\vec{k}}}{|d_{\vec{k}}|} \quad (25)$$

216 of a contractible loop C in the Brillouin zone. A nonzero winding number signifies the presence
217 of a nodal point \mathbf{k}_o within the loop. For this analysis, we assume

$$p(\vec{k}) \sim |\vec{k} - \vec{k}_o|^{2n} \equiv |\vec{q}|^{2n}$$

218 in the vicinity of the nodal point. For a generic nodal point $\mathbf{k}_o \neq \mathbf{0}$, the mean free path is given
219 by

$$l_{\vec{k}} \sim \tau_{\vec{k}} \sim |\vec{q}|^{-2n},$$

220 and the probability distribution becomes:

$$1 = \int p(\vec{q}) d\vec{q}^2 \sim \int q^{2n} q dq \sim \int l^{-2-1/n} dl.$$

221 Consequently, the dynamical exponent is

$$z_n = \frac{n + 1}{n}. \quad (26)$$

222 If the nodal point is situated at one of the high-symmetry points, the mean free path becomes

$$l_{\vec{k}} \sim v_{\vec{k}} \tau_{\vec{k}} \sim |\vec{q}|^{-(2n-1)},$$

223 and the probability distribution can be expressed as

$$1 = \int p(\vec{q}) d\vec{q}^2 \sim \int l^{-2-3/(2n-1)} dl.$$

224 The dynamical exponent in this case is

$$z_n = \frac{2n+2}{2n-1}. \quad (27)$$

225 For superdiffusion in this context, $n \geq 3$ is required; a smaller value of n results in diffusive
226 transport.

227 **3D systems** If time-reversal and reflection symmetry are present, we can similarly define
228 seven indicators, which are the product of \vec{d}_0 and $\vec{d}_{\vec{k}}$ at one of seven high-symmetry points
229 in the Brillouin zone. A negative sign in these indicators implies the presence of a nodal
230 surface. Assuming that the dispersion near the nodal surface is proportional to the orthogonal
231 component: $d_{\vec{k}} \sim k_{\perp}^n$, a similar calculation yields a dynamical exponent of

$$z_n = \frac{2n+1}{2n}. \quad (28)$$

232 Without the symmetry constraint, we can similarly define winding number $W[C]$ for a con-
233 tractible loop C ; a non-zero winding implies a nodal line. Assuming the dispersion relation
234 $d_{\vec{k}} \sim k_{\perp}^n$ near the curve, we obtain a dynamical exponent of

$$z_n = \frac{n+1}{n}. \quad (29)$$

235 5 Conclusion

236 This study uncovered a straightforward yet profound mechanism that leads to superdiffusive
237 transport within noninteracting fermion systems subjected to local dephasing. Our findings
238 demonstrate that we can fundamentally alter the system's behavior by extending the onsite
239 particle dephasing to the dephasing of local quasi-particles featuring nodal points. The dy-
240 namics of a momentum- \vec{k} wave packet in this setting resemble the diffusive particle but with
241 a unique feature: its mean free paths $l_{\vec{k}}$ diverge when the momentum approaches the nodal
242 point:

$$l_{\vec{k}} \sim |\vec{k} - \vec{k}_o|^n. \quad (30)$$

243 By studying the Wigner dynamics of the Lindbladian, we have rigorously mapped the system's
244 behavior to that of a random walk. Notably, this random walk manifests as a *Lévy walk*, a well-
245 established model of superdiffusion in physics. This mapping not only elucidates the physical
246 underpinnings of the observed superdiffusion but also enables us to determine the dynamical
247 exponent governing the system's behavior precisely.

248 Furthermore, it empowers us to design and engineer models with different exact dynamical
249 exponents, broadening our grasp of the phenomenon. It is worth noting that this superdiffusive
250 transport extends naturally to higher dimensions. This generality underscores the universality
251 of the mechanism, offering valuable insights that can be applied across a spectrum of quantum
252 many-body systems.

253 In this work, the initial state of the dynamics is consistently set to the domain wall state

$$|\psi_o\rangle = |1 \cdots 10 \cdots 0\rangle.$$

254 However, the phenomenon of superdiffusion is not confined to this specific initial state. Ac-
 255 cording to the random walk argument, superdiffusive charge transport should also be present
 256 in a generic, imbalanced configuration and in the infinite temperature ensemble. Notably,
 257 further research [58] demonstrates that the model presented in this paper exhibits superdif-
 258 fusion, with the same dynamical exponent, in a boundary driving setup, which is considered
 259 indicative of infinite-temperature transport [1, 59].

260 Additionally, the concept of nodal points in quasi-particles provides a general strategy for
 261 achieving superdiffusion. This concept is extended to disordered systems in Refs. [60, 61],
 262 leading to new types of superdiffusive behaviors.

263 Acknowledgements

264 J.R. and Y.-P. W. thanks Marko Žnidarič for his careful reading of the manuscript and useful
 265 comments and suggestions. The numerical simulation of the Lindblad equation uses the Julia
 266 package `DifferentialEquation.jl` [62].

267 A Closed Hierarchy of the Correlation Function

268 In this section, we will show that the dynamics governed by a Lindbladian consisting of free
 269 fermion Hamiltonian and Hermitian quadratic jump operators can be efficiently simulated due
 270 to a closed hierarchy [53–55] of the correlation function. Specifically, the dynamics of the two-
 271 point correlation function can be formulated as a differential equation that is linear in itself
 272 and does not involve any multi-point correlations.

273 We first consider the Lindblad equation for operators:

$$\partial_t \hat{O} = i[\hat{H}, \hat{O}] - \frac{\gamma}{2} \sum_n [\hat{L}_n [\hat{L}_n, \hat{O}]], \quad (\text{A.1})$$

274 where each jump operator is a Hermitian fermion bilinear:

$$\hat{L}_x = \sum_{ab} d_a^* d_b \hat{c}_{x+a}^\dagger \hat{c}_{x+b} \equiv \sum_{ij} A_{x,ij} \hat{c}_i^\dagger \hat{c}_j, \quad A_{x,ij} = d_{i-x}^* d_{j-x}. \quad (\text{A.2})$$

275 Since we concern only the two-point correlation $G_{ij} = \langle c_i^\dagger c_j \rangle$, we can choose $\hat{O}_{ij} = c_i^\dagger c_j$. Using
 276 the commutation relation $[c_i^\dagger c_j, c_k^\dagger c_l] = \delta_{jk} c_i^\dagger c_l - \delta_{il} c_k^\dagger c_j$, we know the following identity:

$$\sum_{kl} [A_{kl} \hat{c}_k^\dagger \hat{c}_l, \hat{c}_i^\dagger \hat{c}_j] = \sum_k [A_{ki} \hat{c}_k^\dagger \hat{c}_j - \hat{c}_i^\dagger \hat{c}_k A_{jk}]. \quad (\text{A.3})$$

277 We can use the identity to calculate the commutator of two fermion bilinears and obtain the
 278 following:

$$i \sum_{kl} H_{kl} [\hat{c}_k^\dagger \hat{c}_l, \hat{O}_{ij}] = i \sum_{kl} H_{kl} (\delta_{il} \hat{c}_k^\dagger \hat{c}_j - \delta_{jk} \hat{c}_i^\dagger \hat{c}_l) = i[H^T \cdot \hat{O} - \hat{O} \cdot H^T]_{ij}.$$

279 Similarly, the double commutation in the second term is:

$$-\frac{\gamma}{2} \sum_x [\hat{L}_x [\hat{L}_x, \hat{O}_{ij}]] = -\frac{\gamma}{2} \sum_x [(A_x^*)^2 \cdot \hat{O} + \hat{O} \cdot (A_x^*)^2 - 2A_x^* \cdot \hat{O} \cdot A_x^*].$$

280 Together, the EOM of the two-point correlation function is

$$\partial_t \mathbf{G} = \mathbf{X}^\dagger \cdot \mathbf{G} + \mathbf{G} \cdot \mathbf{X} + \gamma \sum_x \mathbf{A}_x^* \cdot \mathbf{G} \cdot \mathbf{A}_x^* \equiv \mathcal{L}[\mathbf{G}], \quad (\text{A.4})$$

281 where $\mathbf{X} = -i\mathbf{H}^* - \frac{\gamma}{2} \sum_x (\mathbf{A}_x^*)^2$.

282 Note that the right-hand side of Eq. (A.4) is linear in \mathbf{G} , the evolution of \mathbf{G} can be formally
283 written as

$$\mathbf{G}(t) = e^{\mathcal{L}t}[\mathbf{G}_0]. \quad (\text{A.5})$$

284 To obtain the trajectory in the numerical simulation, simply implement the $\mathcal{L}[\cdot]$ action and
285 insert the linear operator into a numerical solver for the differential equation.

286 B Effective Hydrodynamics

287 In this appendix, following Refs. [50,51], we derive the Wigner dynamics of quasi-free Lindbladian
288 for general d -dimension. The Hamiltonians are supposed to be the simplest free fermion
289 model on the square lattice:

$$\hat{H} = \sum_{\langle \bar{x}, \bar{y} \rangle} \hat{c}_{\bar{x}}^\dagger \hat{c}_{\bar{y}} + \hat{c}_{\bar{y}}^\dagger \hat{c}_{\bar{x}}. \quad (\text{B.1})$$

290 The Lindblad equation for operator \hat{O} has the form:

$$\partial_t \hat{O} = i[\hat{H}, \hat{O}] - \frac{\gamma}{2} \sum_n [\hat{L}_n [\hat{L}_n, \hat{O}]]. \quad (\text{B.2})$$

291 We are considering the evolution of the operator

$$\hat{n}(\bar{x}, \bar{k}) \equiv \sum_s e^{i\bar{k} \cdot \bar{s}} \hat{c}_{\bar{x} + \frac{\bar{s}}{2}}^\dagger \hat{c}_{\bar{x} - \frac{\bar{s}}{2}}, \quad (\text{B.3})$$

292 The hydrodynamics is then obtained by taking the expectation value: $n(\bar{x}, \bar{k}, t) = \langle \hat{n}(\bar{x}, \bar{k}) \rangle_t$.

293 **Hopping Hamiltonian** We first consider the Hamiltonian part of the Lindbladian. Using the
294 identity

$$[\hat{c}_i^\dagger \hat{c}_j, \hat{c}_k^\dagger \hat{c}_l] = \hat{c}_i^\dagger [\hat{c}_j, \hat{c}_k^\dagger \hat{c}_l] + [\hat{c}_i^\dagger, \hat{c}_k^\dagger \hat{c}_l] \hat{c}_j = \delta_{jk} \hat{c}_i^\dagger \hat{c}_l - \delta_{il} \hat{c}_i^\dagger \hat{c}_j, \quad (\text{B.4})$$

295 we obtain the commutation relation

$$[\hat{H}, \hat{c}_{\bar{x}}^\dagger \hat{c}_{\bar{y}}] = \sum_{i=1}^D \left(\hat{c}_{\bar{x} + \bar{e}_i}^\dagger \hat{c}_{\bar{y}} + \hat{c}_{\bar{x} - \bar{e}_i}^\dagger \hat{c}_{\bar{y}} - \hat{c}_{\bar{x}}^\dagger \hat{c}_{\bar{y} + \bar{e}_i} - \hat{c}_{\bar{x}}^\dagger \hat{c}_{\bar{y} - \bar{e}_i} \right), \quad (\text{B.5})$$

296 where \bar{e}_i is the unit vector for each direction and thus

$$\begin{aligned} i[\hat{H}, \hat{n}(\bar{x}, \bar{k})] &= i \sum_{\bar{s}} e^{i\bar{k} \cdot \bar{s}} \sum_{i=1}^D \left[\hat{c}_{\bar{x} + \frac{\bar{s}}{2} + \bar{e}_i}^\dagger \hat{c}_{\bar{x} - \frac{\bar{s}}{2}} + \hat{c}_{\bar{x} + \frac{\bar{s}}{2} - \bar{e}_i}^\dagger \hat{c}_{\bar{x} - \frac{\bar{s}}{2}} - \hat{c}_{\bar{x} + \frac{\bar{s}}{2}}^\dagger \hat{c}_{\bar{x} - \frac{\bar{s}}{2} + \bar{e}_i} - \hat{c}_{\bar{x} + \frac{\bar{s}}{2}}^\dagger \hat{c}_{\bar{x} - \frac{\bar{s}}{2} - \bar{e}_i} \right] \\ &= 2 \sum_{i=1}^D \sin(k_i) \left[\hat{n} \left(\bar{x} + \frac{\bar{e}_i}{2}, \bar{k} \right) - \hat{n} \left(\bar{x} - \frac{\bar{e}_i}{2}, \bar{k} \right) \right]. \end{aligned}$$

297 In the coarse-grained

$$n \left(\bar{x} + \frac{\bar{e}_i}{2}, \bar{k}, t \right) - n \left(\bar{x} - \frac{\bar{e}_i}{2}, \bar{k}, t \right) \simeq \frac{\partial n}{\partial x_i}(\bar{x}, \bar{k}, t), \quad (\text{B.6})$$

298 So the Hamiltonian part of the hydrodynamics is

$$dn(\bar{x}, \bar{k}, t) = -2 \sum_{i=1}^D \sin(k_i) \frac{\partial n}{\partial x_i}(\bar{x}, \bar{k}, t) dt. \quad (\text{B.7})$$

299 **Dissipation** Here, we consider the dephasing of the local quasi-particle at y ,

$$\hat{L}_y = \sum_{ab} d_a^* d_b \hat{c}_{y+a}^\dagger \hat{c}_{y+b}. \quad (\text{B.8})$$

300 We denote $A_{ab} = d_a^* d_b$, the commutator $[\hat{L}_y, \hat{n}(x, k)]$ is

$$\begin{aligned} [\hat{L}_y, \hat{n}(x, k)] &= \sum_{s, ab} e^{iks} A_{ab} \left[\hat{c}_{y+a}^\dagger \hat{c}_{y+b}, \hat{c}_{x+\frac{s}{2}}^\dagger \hat{c}_{x-\frac{s}{2}} \right] \\ &= \sum_{s, ab} e^{iks} A_{ab} \left[\delta_{y-x+b, \frac{s}{2}} \hat{c}_{y+a}^\dagger \hat{c}_{x-\frac{s}{2}} - \delta_{x-y-a, \frac{s}{2}} \hat{c}_{x+\frac{s}{2}}^\dagger \hat{c}_{y+b} \right] \\ &= \sum_{ab} A_{ab} \left[e^{-2ik(x-y-b)} \hat{c}_{y+a}^\dagger \hat{c}_{2x-y-b} - e^{+2ik(x-y-a)} \hat{c}_{2x-y-a}^\dagger \hat{c}_{y+b} \right]. \end{aligned}$$

301 Using the fact

$$\frac{1}{N} \sum_p e^{-ipx} \hat{n}(x, p) = \frac{1}{N} \sum_p \sum_s e^{ip(s-a)} \hat{c}_{x+\frac{s}{2}}^\dagger \hat{c}_{x-\frac{s}{2}} = \sum_p \delta_{s,a} \hat{c}_{x+\frac{s}{2}}^\dagger \hat{c}_{x-\frac{s}{2}} = \hat{c}_{x+\frac{a}{2}}^\dagger \hat{c}_{x-\frac{a}{2}},$$

302 the result is

$$\begin{aligned} [\hat{L}_y, \hat{n}(x, k)] &= \frac{1}{N} \sum_{ab, p} A_{ab} e^{-ip(a-b)} \\ &\quad \times \left[e^{-2i(k-p)(x-y-b)} \hat{n}\left(x + \frac{a-b}{2}, p\right) - e^{+2i(k-p)(x-y-a)} \hat{n}\left(x - \frac{a-b}{2}, p\right) \right]. \end{aligned}$$

303 For the double commutator $[\hat{L}_y, [\hat{L}_y, \hat{n}(x, k)]]$, we need to replace the Wigner distribution in
304 the right-hand side with $[\hat{L}_y, \hat{n}]$. There are four terms involved:

$$[\hat{L}_y, [\hat{L}_y, \hat{n}(x, k)]] = S_1 + S_2 + S_3 + S_4,$$

305 where S_1 and S_2 come from

$$\hat{n}\left(x + \frac{a-b}{2}, p\right) \rightarrow \left[\hat{L}_y, \hat{n}\left(x + \frac{a-b}{2}, p\right) \right];$$

306 the S_3 and S_4 come from

$$\hat{n}\left(x - \frac{a-b}{2}, p\right) \rightarrow \left[\hat{L}_y, \hat{n}\left(x - \frac{a-b}{2}, p\right) \right].$$

307 In the following, we will simplify the expression term by term. For the first term S_1 ,

$$\begin{aligned} S_1 &= \frac{1}{N^2} \sum_{abcd, pq, y} A_{ab} A_{cd} e^{-ip(a-b)-iq(c-d)} e^{-2i(k-p)(x-y-b)} e^{-2i(p-q)(x+\frac{a-b}{2}-y-d)} \hat{n}\left(x + \frac{a-b+c-d}{2}, q\right) \\ &= \frac{1}{N} \sum_{abcd, pq} \left(\sum_y \frac{e^{2iy(k-q)}}{N} \right) A_{ab} A_{cd} e^{-ip(a-b)-iq(c-d)-2i(k-p)(x-b)} e^{-2i(p-q)(x+\frac{a-b}{2}-d)} \hat{n}\left(x + \frac{a-b+c-d}{2}, q\right) \\ &= \frac{1}{N} \sum_{abcd, pq} \delta_{k,q} A_{ab} A_{cd} e^{-ip(a-b)-iq(c-d)-2i(k-p)(x-b)} e^{-2i(p-q)(x+\frac{a-b}{2}-d)} \hat{n}\left(x + \frac{a-b+c-d}{2}, q\right) \\ &= \frac{1}{N} \sum_{abcd} \sum_p A_{ab} A_{cd} e^{-ip(a-b)-ik(c-d)} e^{2i(k-p)(\frac{a+b}{2}-d)} \hat{n}\left(x + \frac{a-b+c-d}{2}, k\right) \\ &= \sum_{abcd} \left(\frac{1}{N} \sum_p e^{-2ip(a-d)} \right) A_{ab} A_{cd} e^{ik(a+b-c-d)} \hat{n}\left(x + \frac{a-b+c-d}{2}, k\right) \\ &= \sum_{bc} (A^2)_{cb} e^{ik(b-c)} \hat{n}\left(x - \frac{b-c}{2}, k\right). \end{aligned}$$

308 The calculation for S_4 is similar to S_1 :

$$\begin{aligned}
S_4 &= \frac{1}{N^2} \sum_{abcd,pq,y} A_{ab}A_{cd} e^{-ip(a-b)-iq(c-d)} e^{2i(k-p)(x-y-a)} e^{2i(p-q)(x-\frac{a-b}{2}-y-c)} \hat{n}\left(x - \frac{a-b+c-d}{2}, q\right) \\
&= \frac{1}{N} \sum_{abcd,pq} \delta_{k,q} A_{ab}A_{cd} e^{-ip(a-b)-iq(c-d)} e^{2i(k-p)(x-a)} e^{2i(p-q)(x-\frac{a-b}{2}-c)} \hat{n}\left(x - \frac{a-b+c-d}{2}, q\right) \\
&= \frac{1}{N} \sum_{abcd,p} A_{ab}A_{cd} e^{-ip(a-b)-ik(c-d)} e^{i(p-k)(a+b-2c)} \hat{n}\left(x - \frac{a-b+c-d}{2}, k\right) \\
&= \sum_{abcd} \delta_{b,c} A_{ab}A_{cd} e^{-ik(a+b-c-d)} \hat{n}\left(x - \frac{a-b+c-d}{2}, k\right) \\
&= \sum_{ad} (A^2)_{ad} e^{-ik(a-d)} \hat{n}\left(x - \frac{a-d}{2}, k\right).
\end{aligned}$$

309 Since \hat{L}_y is a particle number operator, $\hat{L}_y^2 = \hat{L}_y$, i.e., $A^2 = A$. Moreover, in the coarse-grained
310 limit, we can approximate $\hat{n}(x - (b-c)/2, k)$ and $\hat{n}(x - (a-d)/2, k)$ with $\hat{n}(x, k)$. Therefore,

$$S_1 = S_4 = \sum_a d_a^* e^{-ika} \sum_b d_b e^{ikb} \hat{n}(x, k) = |d_k|^2 \hat{n}(x, k).$$

311 Now we consider the S_2 part:

$$\begin{aligned}
S_2 &= -\frac{1}{N^2} \sum_{abcd,pq,y} A_{ab}A_{cd} e^{-ip(a-b)-iq(c-d)} e^{-2i(k-p)(x-y-b)} e^{2i(p-q)(x+\frac{a-b}{2}-y-c)} \hat{n}\left(x + \frac{a-b-c+d}{2}, q\right) \\
&= -\frac{1}{N} \sum_{abcd,pq} \left(\sum_y \frac{e^{2iy(k-2p+q)}}{N} \right) A_{ab}A_{cd} e^{-ip(a-b)-iq(c-d)-2i(k-p)(x-b)} e^{2i(p-q)(x+\frac{a-b}{2}-c)} \hat{n}\left(x + \frac{a-b-c+d}{2}, q\right) \\
&= -\frac{1}{N} \sum_{abcd,p} A_{ab}A_{cd} e^{-ip(a-b)-i(2p-k)(c-d)} e^{i(k-p)(a+b-2c)} \hat{n}\left(x + \frac{a-b-c+d}{2}, 2p-k\right) \\
&= -\sum_{abcd} \left(\sum_p \frac{e^{-2ip(a-d)}}{N} \right) A_{ab}A_{cd} e^{ik(a+b-c-d)} \hat{n}\left(x + \frac{a-b-c+d}{2}, 2p-k\right) \\
&= -\sum_{abcd} A_{ab}A_{cd} e^{ik(b-c)} \frac{1}{N} \sum_q e^{-iq(a-d)} \hat{n}\left(x + \frac{a-b-c+d}{2}, q\right).
\end{aligned}$$

312 Using the coarse-graining approximation and replacing the momentum sum with the integral,
313 we have:

$$S_2 \simeq -\sum_{bc} d_b d_c^* e^{ik(b-c)} \int \frac{d^D q}{(2\pi)^D} \sum_{ad} d_a^* d_a e^{-iq(a-d)} \hat{n}(x, q) = -|d_k|^2 \int \frac{d^D q}{(2\pi)^D} |d_q|^2 \hat{n}(x, q).$$

314 Straightforward calculation shows $S_3 \simeq S_2$:

$$\begin{aligned}
S_3 &= -\frac{1}{N^2} \sum_{abcd,pq,y} A_{ab}A_{cd} e^{-ip(a-b)-iq(c-d)} e^{2i(k-p)(x-y-a)} e^{-2i(p-q)(x+\frac{a-b}{2}-y-d)} \hat{n}\left(x - \frac{a-b-c+d}{2}, q\right) \\
&= -\frac{1}{N} \sum_{abcd,pq} \delta_{q,2p-k} A_{ab}A_{cd} e^{-ip(a-b)-iq(c-d)} e^{2i(k-p)(x-a)} e^{-2i(p-q)(x-\frac{a-b}{2}-d)} \hat{n}\left(x - \frac{a-b-c+d}{2}, q\right) \\
&= -\sum_{abcd} A_{ab}A_{cd} e^{-ik(a+b-c-d)} \int \frac{d^D q}{(2\pi)^D} e^{2ip(b-c)} \hat{n}\left(x - \frac{a-b-c+d}{2}, 2p-k\right) \\
&= -\sum_{abcd} A_{ab}A_{cd} e^{-ik(a-d)} \int \frac{d^D q}{(2\pi)^D} e^{iq(b-c)} \hat{n}\left(x - \frac{a-b-c+d}{2}, q\right) \\
&\simeq -|d_k|^2 \int \frac{d^D q}{(2\pi)^D} |d_q|^2 \hat{n}(x, q).
\end{aligned}$$

315 Therefore, we have proved that the hydrodynamics of the Wigner distribution is

$$\partial_t n(\vec{x}, \vec{k}) = -2 \sum_{i=1}^D \sin(k_i) \partial_{x_i} n(\vec{x}, \vec{k}) - \gamma |d_{\vec{k}}|^2 n(\vec{x}, \vec{k}) + \gamma |d_{\vec{k}}|^2 \int \frac{d^D q}{(2\pi)^D} |d_{\vec{q}}|^2 n(\vec{x}, \vec{q}). \quad (\text{B.9})$$

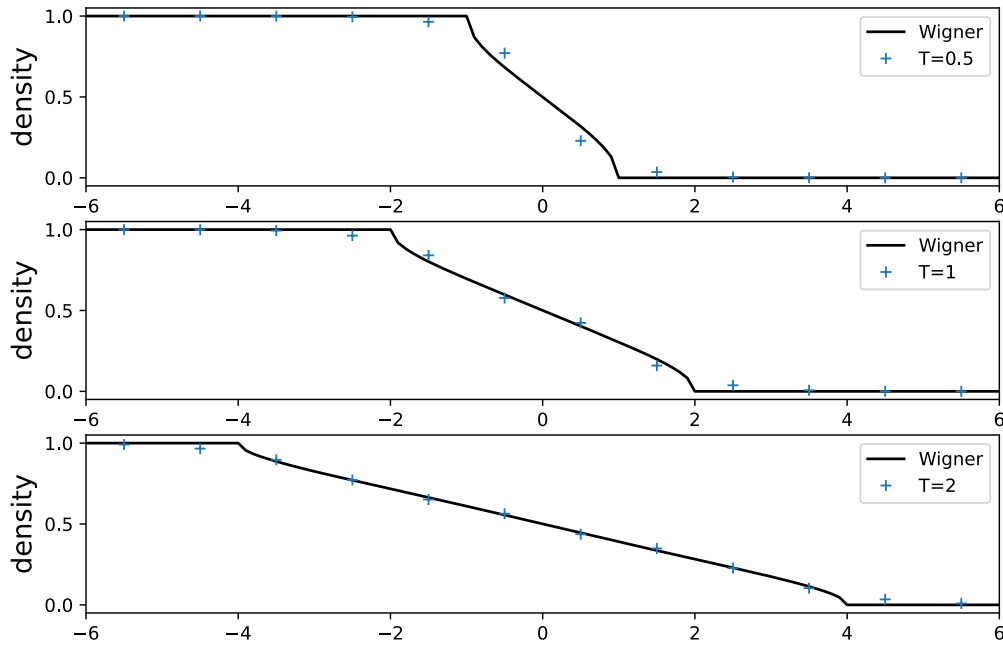


Figure 4: Comparison of the Lindblad equation (C.1) and the Wigner dynamics (B.9) at $T = 0.5, 1, 2$, with $a = \sqrt{2}$ and $\gamma = 0.5$. The markers show the results from the Lindblad equation, and the solid line represents the results of Wigner dynamics.

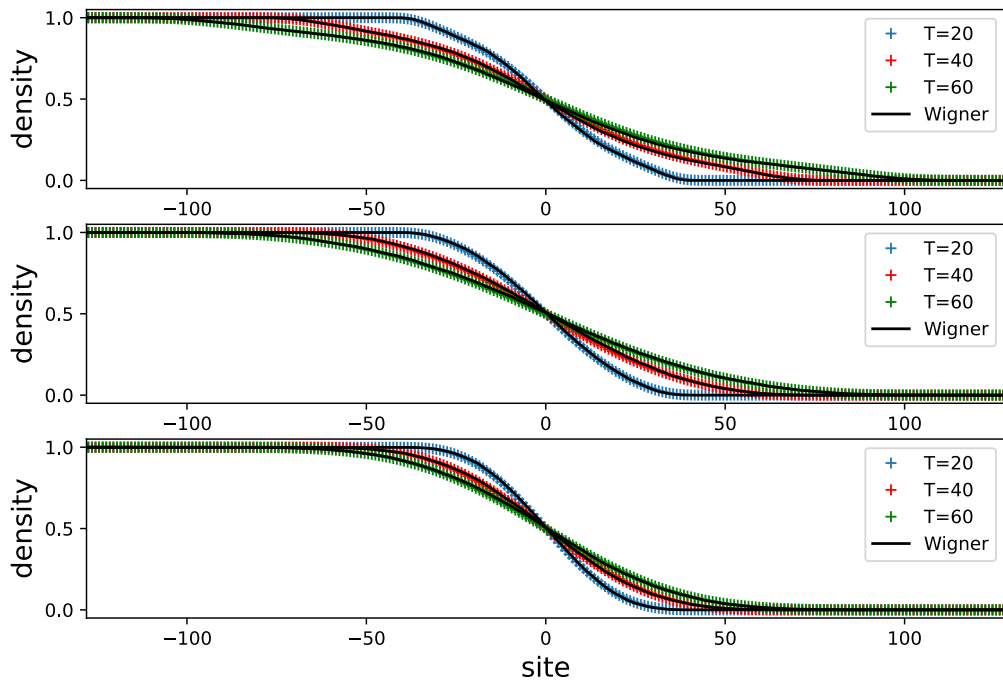


Figure 5: Comparison of the Lindblad equation (C.1) and the Wigner dynamics (B.9) at $T = 20, 40, 60$, with $a = \sqrt{2}$ (top), $a = 2$ (middle), $a = 3$ (bottom), and $\gamma = 0.5$. The markers show the results from the Lindblad equation, and the solid line represents the results of Wigner dynamics.

316 C Comparison between Exact Lindblad and Wigner Dynamics

317 In this appendix, we compare the exact Lindblad dynamics

$$\frac{\partial \rho}{\partial t} = -i[\hat{H}, \rho] - \frac{\gamma}{2} \sum_x [\hat{d}_x^\dagger \hat{d}_x, [\hat{d}_x^\dagger \hat{d}_x, \rho]] \quad (\text{C.1})$$

318 with the Wigner dynamics Eq. (B.9).

319 In terms of the dynamics of the density, we first notice that at short times, as shown in fig. 4
320 for quasiparticle

$$\hat{d}_x = \frac{1}{2} (\hat{c}_{x-1} - \sqrt{2}\hat{c}_x + \hat{c}_{x+1}), \quad (\text{C.2})$$

321 There are certain disagreements between the Lindblad dynamics and the Wigner dynamics.
322 However, as time grows, the disagreements become less prominent.

323 The comparison at later times ($t = 20, 40, 60$), as displayed in Fig. 5 for quasiparticles

$$\hat{d}_x = \frac{1}{\sqrt{2+a^2}} (\hat{c}_{x-1} - a\hat{c}_x + \hat{c}_{x+1}), \quad a = \sqrt{2}, 2, 3 \quad (\text{C.3})$$

324 discussed in the main text shows good agreement.

325 References

- 326 [1] B. Bertini, F. Heidrich-Meisner, C. Karrasch, T. Prosen, R. Steinigeweg and M. Žnidarič,
327 *Finite-temperature transport in one-dimensional quantum lattice models*, Rev. Mod. Phys.
328 **93**, 025003 (2021), doi:[10.1103/RevModPhys.93.025003](https://doi.org/10.1103/RevModPhys.93.025003).
- 329 [2] J. Sirker, *Transport in one-dimensional integrable quantum systems*, SciPost Phys. Lect.
330 Notes p. 17 (2020), doi:[10.21468/SciPostPhysLectNotes.17](https://doi.org/10.21468/SciPostPhysLectNotes.17).
- 331 [3] M. Medenjak, K. Klobas and T. c. v. Prosen, *Diffusion in deterministic interacting lattice*
332 *systems*, Phys. Rev. Lett. **119**, 110603 (2017), doi:[10.1103/PhysRevLett.119.110603](https://doi.org/10.1103/PhysRevLett.119.110603).
- 333 [4] A. Dhar, *Heat transport in low-dimensional systems*, Advances in Physics
334 **57**(5), 457 (2008), doi:[10.1080/00018730802538522](https://doi.org/10.1080/00018730802538522), [https://doi.org/10.1080/](https://doi.org/10.1080/00018730802538522)
335 [00018730802538522](https://doi.org/10.1080/00018730802538522).
- 336 [5] P. Cipriani, S. Denisov and A. Politi, *From anomalous energy diffusion to levy walks*
337 *and heat conductivity in one-dimensional systems*, Phys. Rev. Lett. **94**, 244301 (2005),
338 doi:[10.1103/PhysRevLett.94.244301](https://doi.org/10.1103/PhysRevLett.94.244301).
- 339 [6] S. Chen, J. Wang, G. Casati and G. Benenti, *Nonintegrability and the fourier heat conduc-*
340 *tion law*, Phys. Rev. E **90**, 032134 (2014), doi:[10.1103/PhysRevE.90.032134](https://doi.org/10.1103/PhysRevE.90.032134).
- 341 [7] A. Nahum, J. Ruhman, S. Vijay and J. Haah, *Quantum entanglement growth under random*
342 *unitary dynamics*, Phys. Rev. X **7**, 031016 (2017), doi:[10.1103/PhysRevX.7.031016](https://doi.org/10.1103/PhysRevX.7.031016).
- 343 [8] A. Nahum, S. Vijay and J. Haah, *Operator spreading in random unitary circuits*, Phys.
344 Rev. X **8**, 021014 (2018), doi:[10.1103/PhysRevX.8.021014](https://doi.org/10.1103/PhysRevX.8.021014).
- 345 [9] T. Rakovszky, F. Pollmann and C. W. von Keyserlingk, *Diffusive hydrodynamics of out-*
346 *of-time-ordered correlators with charge conservation*, Phys. Rev. X **8**, 031058 (2018),
347 doi:[10.1103/PhysRevX.8.031058](https://doi.org/10.1103/PhysRevX.8.031058).

- 348 [10] V. Khemani, A. Vishwanath and D. A. Huse, *Operator spreading and the emergence of*
349 *dissipative hydrodynamics under unitary evolution with conservation laws*, Phys. Rev. X **8**,
350 031057 (2018), doi:[10.1103/PhysRevX.8.031057](https://doi.org/10.1103/PhysRevX.8.031057).
- 351 [11] C. W. von Keyserlingk, T. Rakovszky, F. Pollmann and S. L. Sondhi, *Operator hydrody-*
352 *namics, otocs, and entanglement growth in systems without conservation laws*, Phys. Rev.
353 X **8**, 021013 (2018), doi:[10.1103/PhysRevX.8.021013](https://doi.org/10.1103/PhysRevX.8.021013).
- 354 [12] T. Zhou, S. Xu, X. Chen, A. Guo and B. Swingle, *Operator lévy flight: Light*
355 *cones in chaotic long-range interacting systems*, Phys. Rev. Lett. **124**, 180601 (2020),
356 doi:[10.1103/PhysRevLett.124.180601](https://doi.org/10.1103/PhysRevLett.124.180601).
- 357 [13] V. B. Bulchandani, S. Gopalakrishnan and E. Ilievski, *Superdiffusion in spin chains*,
358 Journal of Statistical Mechanics: Theory and Experiment **2021**(8), 084001 (2021),
359 doi:[10.1088/1742-5468/ac12c7](https://doi.org/10.1088/1742-5468/ac12c7).
- 360 [14] M. Schulz, S. R. Taylor, A. Scardicchio and M. Žnidarič, *Phenomenology of anomalous*
361 *transport in disordered one-dimensional systems*, Journal of Statistical Mechanics: Theory
362 and Experiment **2020**(2), 023107 (2020), doi:[10.1088/1742-5468/ab6de0](https://doi.org/10.1088/1742-5468/ab6de0).
- 363 [15] M. Žnidarič, *Spin transport in a one-dimensional anisotropic heisenberg model*, Phys. Rev.
364 Lett. **106**, 220601 (2011), doi:[10.1103/PhysRevLett.106.220601](https://doi.org/10.1103/PhysRevLett.106.220601).
- 365 [16] M. Ljubotina, M. Žnidarič and T. Prosen, *Spin diffusion from an inhomogeneous*
366 *quench in an integrable system*, Nature Communications **8**(1), 16117 (2017),
367 doi:[10.1038/ncomms16117](https://doi.org/10.1038/ncomms16117).
- 368 [17] M. Ljubotina, M. Žnidarič and T. c. v. Prosen, *Kardar-parisi-zhang physics*
369 *in the quantum heisenberg magnet*, Phys. Rev. Lett. **122**, 210602 (2019),
370 doi:[10.1103/PhysRevLett.122.210602](https://doi.org/10.1103/PhysRevLett.122.210602).
- 371 [18] V. B. Bulchandani, R. Vasseur, C. Karrasch and J. E. Moore, *Bethe-boltzmann hy-*
372 *drodynamics and spin transport in the xxz chain*, Phys. Rev. B **97**, 045407 (2018),
373 doi:[10.1103/PhysRevB.97.045407](https://doi.org/10.1103/PhysRevB.97.045407).
- 374 [19] A. Scheie, N. E. Sherman, M. Dupont, S. E. Nagler, M. B. Stone, G. E. Granroth, J. E.
375 Moore and D. A. Tennant, *Detection of kardar–parisi–zhang hydrodynamics in a quantum*
376 *heisenberg spin-1/2 chain*, Nature Physics **17**(6), 726 (2021), doi:[10.1038/s41567-021-](https://doi.org/10.1038/s41567-021-01191-6)
377 [01191-6](https://doi.org/10.1038/s41567-021-01191-6).
- 378 [20] J. De Nardis, M. Medenjak, C. Karrasch and E. Ilievski, *Anomalous spin diffu-*
379 *sion in one-dimensional antiferromagnets*, Phys. Rev. Lett. **123**, 186601 (2019),
380 doi:[10.1103/PhysRevLett.123.186601](https://doi.org/10.1103/PhysRevLett.123.186601).
- 381 [21] S. Gopalakrishnan and R. Vasseur, *Kinetic theory of spin diffusion and su-*
382 *perdiffusion in xxz spin chains*, Phys. Rev. Lett. **122**, 127202 (2019),
383 doi:[10.1103/PhysRevLett.122.127202](https://doi.org/10.1103/PhysRevLett.122.127202).
- 384 [22] J. De Nardis, S. Gopalakrishnan, E. Ilievski and R. Vasseur, *Superdiffusion from emer-*
385 *gent classical solitons in quantum spin chains*, Phys. Rev. Lett. **125**, 070601 (2020),
386 doi:[10.1103/PhysRevLett.125.070601](https://doi.org/10.1103/PhysRevLett.125.070601).
- 387 [23] M. Kardar, G. Parisi and Y.-C. Zhang, *Dynamic scaling of growing interfaces*, Phys. Rev.
388 Lett. **56**, 889 (1986), doi:[10.1103/PhysRevLett.56.889](https://doi.org/10.1103/PhysRevLett.56.889).

- 389 [24] I. CORWIN, *The kardar–parisi–zhang equation and universality class*, Random Matrices:
390 Theory and Applications **01**(01), 1130001 (2012), doi:[10.1142/S2010326311300014](https://doi.org/10.1142/S2010326311300014),
391 <https://doi.org/10.1142/S2010326311300014>.
- 392 [25] M. Prähofer and H. Spohn, *Exact scaling functions for one-dimensional sta-*
393 *tionary kpz growth*, Journal of Statistical Physics **115**(1), 255 (2004),
394 doi:[10.1023/B:JOSS.0000019810.21828.fc](https://doi.org/10.1023/B:JOSS.0000019810.21828.fc).
- 395 [26] M. Dupont and J. E. Moore, *Universal spin dynamics in infinite-temperature*
396 *one-dimensional quantum magnets*, Phys. Rev. B **101**, 121106 (2020),
397 doi:[10.1103/PhysRevB.101.121106](https://doi.org/10.1103/PhysRevB.101.121106).
- 398 [27] Žiga Krajnik, E. Ilievski and T. Prosen, *Integrable matrix models in discrete space-time*,
399 SciPost Phys. **9**, 038 (2020), doi:[10.21468/SciPostPhys.9.3.038](https://doi.org/10.21468/SciPostPhys.9.3.038).
- 400 [28] Ž. Krajnik and T. Prosen, *Kardar–parisi–zhang physics in integrable rotationally symmetric*
401 *dynamics on discrete space–time lattice*, Journal of Statistical Physics **179**(1), 110 (2020),
402 doi:[10.1007/s10955-020-02523-1](https://doi.org/10.1007/s10955-020-02523-1).
- 403 [29] M. Fava, B. Ware, S. Gopalakrishnan, R. Vasseur and S. A. Parameswaran, *Spin crossovers*
404 *and superdiffusion in the one-dimensional hubbard model*, Phys. Rev. B **102**, 115121
405 (2020), doi:[10.1103/PhysRevB.102.115121](https://doi.org/10.1103/PhysRevB.102.115121).
- 406 [30] E. Ilievski, J. De Nardis, S. Gopalakrishnan, R. Vasseur and B. Ware, *Superuniversality of*
407 *superdiffusion*, Phys. Rev. X **11**, 031023 (2021), doi:[10.1103/PhysRevX.11.031023](https://doi.org/10.1103/PhysRevX.11.031023).
- 408 [31] B. Ye, F. Machado, J. Kemp, R. B. Hutson and N. Y. Yao, *Universal kardar-parisi-*
409 *zhang dynamics in integrable quantum systems*, Phys. Rev. Lett. **129**, 230602 (2022),
410 doi:[10.1103/PhysRevLett.129.230602](https://doi.org/10.1103/PhysRevLett.129.230602).
- 411 [32] A. J. Friedman, S. Gopalakrishnan and R. Vasseur, *Diffusive hydrodynamics from integra-*
412 *bility breaking*, Phys. Rev. B **101**, 180302 (2020), doi:[10.1103/PhysRevB.101.180302](https://doi.org/10.1103/PhysRevB.101.180302).
- 413 [33] J. De Nardis, S. Gopalakrishnan, R. Vasseur and B. Ware, *Stability of superdif-*
414 *fusion in nearly integrable spin chains*, Phys. Rev. Lett. **127**, 057201 (2021),
415 doi:[10.1103/PhysRevLett.127.057201](https://doi.org/10.1103/PhysRevLett.127.057201).
- 416 [34] P. W. Claeys, A. Lamacraft and J. Herzog-Arbeitman, *Absence of superdiffu-*
417 *sion in certain random spin models*, Phys. Rev. Lett. **128**, 246603 (2022),
418 doi:[10.1103/PhysRevLett.128.246603](https://doi.org/10.1103/PhysRevLett.128.246603).
- 419 [35] D. Roy, A. Dhar, H. Spohn and M. Kulkarni, *Robustness of kardar-parisi-zhang scaling*
420 *in a classical integrable spin chain with broken integrability*, Phys. Rev. B **107**, L100413
421 (2023), doi:[10.1103/PhysRevB.107.L100413](https://doi.org/10.1103/PhysRevB.107.L100413).
- 422 [36] A. D. Mirlin, Y. V. Fyodorov, F.-M. Dittes, J. Quezada and T. H. Seligman, *Transition from*
423 *localized to extended eigenstates in the ensemble of power-law random banded matrices*,
424 Phys. Rev. E **54**, 3221 (1996), doi:[10.1103/PhysRevE.54.3221](https://doi.org/10.1103/PhysRevE.54.3221).
- 425 [37] V. K. Varma, C. de Mulatier and M. Žnidarič, *Fractality in nonequilib-*
426 *rium steady states of quasiperiodic systems*, Phys. Rev. E **96**, 032130 (2017),
427 doi:[10.1103/PhysRevE.96.032130](https://doi.org/10.1103/PhysRevE.96.032130).
- 428 [38] M. Saha, S. K. Maiti and A. Purkayastha, *Anomalous transport through alge-*
429 *braically localized states in one dimension*, Phys. Rev. B **100**, 174201 (2019),
430 doi:[10.1103/PhysRevB.100.174201](https://doi.org/10.1103/PhysRevB.100.174201).

- 431 [39] A. Schuckert, I. Lovas and M. Knap, *Nonlocal emergent hydrodynamics*
432 *in a long-range quantum spin system*, Phys. Rev. B **101**, 020416 (2020),
433 doi:[10.1103/PhysRevB.101.020416](https://doi.org/10.1103/PhysRevB.101.020416).
- 434 [40] J. Richter, O. Lunt and A. Pal, *Transport and entanglement growth in*
435 *long-range random clifford circuits*, Phys. Rev. Res. **5**, L012031 (2023),
436 doi:[10.1103/PhysRevResearch.5.L012031](https://doi.org/10.1103/PhysRevResearch.5.L012031).
- 437 [41] M. K. Joshi, F. Kranzl, A. Schuckert, I. Lovas, C. Maier, R. Blatt, M. Knap and C. F.
438 Roos, *Observing emergent hydrodynamics in a long-range quantum magnet*, Science
439 **376**(6594), 720 (2022), doi:[10.1126/science.abk2400](https://doi.org/10.1126/science.abk2400), <https://www.science.org/doi/pdf/10.1126/science.abk2400>.
- 441 [42] Y. Yoo, J. Lee and B. Swingle, *Nonequilibrium steady state phases of the*
442 *interacting aubry-andré-harper model*, Phys. Rev. B **102**, 195142 (2020),
443 doi:[10.1103/PhysRevB.102.195142](https://doi.org/10.1103/PhysRevB.102.195142).
- 444 [43] Y. B. Lev, D. M. Kennes, C. Klöckner, D. R. Reichman and C. Karrasch, *Transport in*
445 *quasiperiodic interacting systems: From superdiffusion to subdiffusion*, Europhysics Letters
446 **119**(3), 37003 (2017), doi:[10.1209/0295-5075/119/37003](https://doi.org/10.1209/0295-5075/119/37003).
- 447 [44] M. Žnidarič, *Comment on “nonequilibrium steady state phases of the in-*
448 *teracting aubry-andré-harper model”*, Phys. Rev. B **103**, 237101 (2021),
449 doi:[10.1103/PhysRevB.103.237101](https://doi.org/10.1103/PhysRevB.103.237101).
- 450 [45] A. Bastianello, J. De Nardis and A. De Luca, *Generalized hydrodynamics with dephasing*
451 *noise*, Phys. Rev. B **102**, 161110 (2020), doi:[10.1103/PhysRevB.102.161110](https://doi.org/10.1103/PhysRevB.102.161110).
- 452 [46] X. Turkeshi and M. Schiró, *Diffusion and thermalization in a boundary-driven dephasing*
453 *model*, Phys. Rev. B **104**, 144301 (2021), doi:[10.1103/PhysRevB.104.144301](https://doi.org/10.1103/PhysRevB.104.144301).
- 454 [47] T. Jin, J. a. S. Ferreira, M. Filippone and T. Giamarchi, *Exact description of quan-*
455 *tum stochastic models as quantum resistors*, Phys. Rev. Res. **4**, 013109 (2022),
456 doi:[10.1103/PhysRevResearch.4.013109](https://doi.org/10.1103/PhysRevResearch.4.013109).
- 457 [48] T. Jin, J. a. Ferreira, M. Bauer, M. Filippone and T. Giamarchi, *Semiclassical*
458 *theory of quantum stochastic resistors*, Phys. Rev. Res. **5**, 013033 (2023),
459 doi:[10.1103/PhysRevResearch.5.013033](https://doi.org/10.1103/PhysRevResearch.5.013033).
- 460 [49] T. Jin, J. a. S. Ferreira, M. Filippone and T. Giamarchi, *Exact description of quan-*
461 *tum stochastic models as quantum resistors*, Phys. Rev. Res. **4**, 013109 (2022),
462 doi:[10.1103/PhysRevResearch.4.013109](https://doi.org/10.1103/PhysRevResearch.4.013109).
- 463 [50] X. Cao, A. Tilloy and A. D. Luca, *Entanglement in a fermion chain under continuous*
464 *monitoring*, SciPost Phys. **7**, 024 (2019), doi:[10.21468/SciPostPhys.7.2.024](https://doi.org/10.21468/SciPostPhys.7.2.024).
- 465 [51] M. Coppola, G. T. Landi and D. Karevski, *Wigner dynamics for quantum gases under*
466 *inhomogeneous gain and loss processes with dephasing*, Phys. Rev. A **107**, 052213 (2023),
467 doi:[10.1103/PhysRevA.107.052213](https://doi.org/10.1103/PhysRevA.107.052213).
- 468 [52] V. Zaburdaev, S. Denisov and J. Klafter, *Lévy walks*, Rev. Mod. Phys. **87**, 483 (2015),
469 doi:[10.1103/RevModPhys.87.483](https://doi.org/10.1103/RevModPhys.87.483).
- 470 [53] M. Žnidarič, *Exact solution for a diffusive nonequilibrium steady state of an open quan-*
471 *tum chain*, Journal of Statistical Mechanics: Theory and Experiment **2010**(05), L05002
472 (2010), doi:[10.1088/1742-5468/2010/05/L05002](https://doi.org/10.1088/1742-5468/2010/05/L05002).

- 473 [54] V. Eisler, *Crossover between ballistic and diffusive transport: the quantum exclusion process*,
474 *Journal of Statistical Mechanics: Theory and Experiment* **2011**(06), P06007 (2011),
475 doi:[10.1088/1742-5468/2011/06/P06007](https://doi.org/10.1088/1742-5468/2011/06/P06007).
- 476 [55] B. Žunkovič, *Closed hierarchy of correlations in markovian open quantum systems*, *New*
477 *Journal of Physics* **16**(1), 013042 (2014), doi:[10.1088/1367-2630/16/1/013042](https://doi.org/10.1088/1367-2630/16/1/013042).
- 478 [56] M. Hinarejos, A. Pérez and M. C. Bañuls, *Wigner function for a particle in an in-*
479 *finite lattice*, *New Journal of Physics* **14**(10), 103009 (2012), doi:[10.1088/1367-](https://doi.org/10.1088/1367-2630/14/10/103009)
480 [2630/14/10/103009](https://doi.org/10.1088/1367-2630/14/10/103009).
- 481 [57] Y.-P. Wang, C. Fang and J. Ren, *Absence of entanglement transition due to feedback-induced*
482 *skin effect* (2023), [2209.11241](https://arxiv.org/abs/2209.11241).
- 483 [58] M. Žnidarič, *Superdiffusive magnetization transport in the xx spin chain with nonlocal*
484 *dephasing*, *Phys. Rev. B* **109**, 075105 (2024), doi:[10.1103/PhysRevB.109.075105](https://doi.org/10.1103/PhysRevB.109.075105).
- 485 [59] G. T. Landi, D. Poletti and G. Schaller, *Nonequilibrium boundary-driven quantum*
486 *systems: Models, methods, and properties*, *Rev. Mod. Phys.* **94**, 045006 (2022),
487 doi:[10.1103/RevModPhys.94.045006](https://doi.org/10.1103/RevModPhys.94.045006).
- 488 [60] Y.-P. Wang, J. Ren and C. Fang, *Superdiffusive transport on lattices with nodal impurities*
489 (2024), [2404.16927](https://arxiv.org/abs/2404.16927).
- 490 [61] J. M. Bhat, *Super-diffusive transport in two-dimensional fermionic wires* (2024), [2405.](https://arxiv.org/abs/2405.15560)
491 [15560](https://arxiv.org/abs/2405.15560).
- 492 [62] C. Rackauckas and Q. Nie, *DifferentialEquations.jl—a performant and feature-rich ecosys-*
493 *tem for solving differential equations in Julia*, *Journal of Open Research Software* **5**(1)
494 (2017).